

Model for speed performance of quantum-dot waveguide photodiode

© A.E. Zhukov¹, N.V. Kryzhanovskaya¹, I.S. Makhov¹, E.I. Moiseev¹, A.M. Nadtochiy¹, N.A. Fominykh¹, S.A. Mintairov², N.A. Kalyuzhyy², F.I. Zubov³, M.V. Maximov³

¹ National Research University Higher School of Economics,
190008 St. Petersburg, Russia

² Ioffe Institute,
194021 St. Petersburg, Russia

³ Alferov Federal State Budgetary Institution of Higher Education and Science
Saint Petersburg National Research Academic University of the Russian Academy of Sciences,
194021 St. Petersburg, Russia

E-mail: zhukale@gmail.com, aezhukov@hse.ru

Received April 6, 2023

Revised May 4, 2023

Accepted May 4, 2023

A model is proposed that makes it possible to analytically analyze the speed performance of a waveguide $p-i-n$ photodiode with a light-absorbing region representing a multilayered array of quantum dots separated by undoped spacers. It is shown that there is an optimal number of layers of quantum dots, as well as an optimal thickness of the spacers, which provide the widest bandwidth. The possibility of achieving a frequency range (at the level of -3 dB) above 20 GHz for waveguide photodiodes based on InGaAs/GaAs quantum well-dots is shown

Keywords: photodiode, quantum dots, speed.

DOI: 10.21883/SC.2023.03.56238.4783

1. Introduction

In recent years, much attention has been paid to the development of photodiodes (PD), the light-absorbing area of which is an array of quantum dots (QD). This is due to the opportunity of expanding the spectral range of sensitivity due to the use of QD in comparison with PD based on bulk materials, as well as the success of lasers based on QD, which, together with PD with the same active area, can form an optocoupler with a matched operating wavelength [1,2]. Another advantage of QD-based PD is their extremely low ($\mu\text{A}/\text{cm}^2$) [3–6] dark currents. In $p-i-n$ PD based on QD of the $1.3\ \mu\text{m}$ spectral range, the operating frequency $f_{-3\text{ dB}} = 5.5\ \text{GHz}$ [3] was achieved. The avalanche QD PD of the same spectral range demonstrated the record frequency $f_{-3\text{ dB}} = 20\ \text{GHz}$ [7]. Of particular interest are PD capable of operating in the $0.9\text{--}1.1\ \mu\text{m}$ spectral range, which is in demand in various applications, such as machine vision systems, biometrics, material processing, various surgical and aesthetic medical applications, range finding, IR illumination etc. d. Meanwhile, in the specified range, a decrease in the sensitivity of both InGaAs/InP (in the short-wavelength limit) and GaAs and Si (in the long-wavelength limit) is observed. With the use of multilayer arrays of InGaAs/GaAs QDs, resonant PD were created at a wavelength of $1.06\ \mu\text{m}$ [8] and $1.03\ \mu\text{m}$ [9], but there is no information on their speed. Recently, we have demonstrated $p-i-n$ PD with a light-absorbing active region in the form of multilayer dense arrays of InGaAs QD (the so-called quantum well dots, QWD), for which the maximum speed of 8.2 GHz was obtained in planar [5] and 5.6 GHz in waveguide [6] geometry.

A feature of self-organizing QD is the need to use interlayers of an unstrained material (for example, GaAs) separating layers QD — so-called spacers that prevent plastic relaxation of elastic stresses in a multilayer structure. Increasing the spacer thickness makes it possible to use a larger number of QD rows, causing an increase in absorption, but leads, however, to a change in the thickness of the depletion area. The advantage of the waveguide PD geometry is the lateral input of radiation, which is preferable for the implementation of various optoelectronic integrated circuits, as well as the possibility of increasing the degree of light absorption compared to normal incidence due to the use of longer PD. The latter at the same time increases the capacity and, as a result, reduces the performance. In addition to the RC time constant, the QD PD speed is affected by the escape of charge carriers from QD [10], as well as their drift through the depletion area. It was recently found [5] that the drift velocity of photogenerated carriers decreases in an $p-i-n$ structure containing a multilayer array of QD compared to transport in a similar structure without QD. Taking these processes into account, optimizing the design of a QD PD to achieve the maximum speed seems to be a rather difficult task.

In this paper, based on model concepts and available experimental data, we consider the effect of the number of QD rows and the thickness of the spacer layers between them on the limiting speed of a waveguide PD. Calculations are carried out for waveguide PD with an active area based on InGaAs multilayer quantum well dots with spectral sensitivity in the wavelength range $0.9\text{--}1.1\ \mu\text{m}$, and the opportunity of achieving a frequency response of $> 25\ \text{GHz}$ for detecting light corresponding to the maximum spectral

sensitivity and > 15 GHz for wavelengths at the edge of the sensitivity area.

2. Model

The PD structure considered in this paper contains N_{QD} QD layers separated by d_{sp} spacer layers placed inside the i -region of the $p-i-n$ heterostructure (Fig. 1). It is convenient to express the total thickness d of the i -region in units of d_{sp} so that $d = (N_{\text{QD}} + N_{\text{side}})d_{\text{sp}}$. Here, $N_{\text{QD}} - 1$ characterizes the total thickness i of the spacer interlayers located between the extreme layers of the QD, and $N_{\text{side}} + 1$ — the total thickness of the layers lying between the doped regions and the layers of the QD closest to them (as a rule, N_{side} , which can be a fractional number, is small and is $1-3$).

The speed of operation of light-absorbing devices with a quantum-well active area is affected by the escape of photogenerated charge carriers from the active region into the matrix [11], after which they are carried out by the electric field. We assume that the charge carrier that has passed through the chain participates in the escape process once, so the ejection time t_{esc} is assumed to be independent of the number of QD rows. In [10] a model was proposed that describes the process of hole escape from QD by tunneling through an intermediate state, which can be the wetting layer state. It was shown in [1] that this model well describes the behavior of PD based on InAs/InGaAs QD. The model predicts the following dependence of the escape time t_{esc} on the electric field strength F :

$$t_{\text{esc}} = t_{\infty} \exp\left(\frac{F_0}{F}\right). \quad (1)$$

Here t_{∞} — ejection time in strong fields such as $F \gg F_0$. The F_0 parameter depends on the effective mass of holes and the energy of the intermediate state involved in tunneling: $t_{\infty} = 10$ ps and $F_0 = 12$ kV/cm were determined for InGaAs QWS in [5]. We take into account that $F = (U + \Phi)/d$, where U — reverse voltage, Φ — built-in potential of the $p-i-n$ diode. Thus, when the thickness of the i -region is on the order of a micrometer, the escape time practically ceases to depend on U , being approximately equal to t_{∞} , starting from approximately 10 V (Fig. 2).

In such fields, charge carriers move in GaAs with velocities close to their saturated values v_{sat} , which in a lightly doped material are $\sim 9 \cdot 10^6$ cm/s for both electrons and holes [12]. Thus, the drift time of t_{drift} through a depletion region of $\sim 1 \mu\text{m}$ thickness could be $d/v_{\text{sat}} \sim 10$ ps, which is close to the delay associated with the escape. However, the experimental data [5] point to a slowdown in the vertical transport of charge carriers in GaAs, in which QWD layers are inserted. For example, in the case of a PD containing 20 InGaAs QWD layers in an i GaAs layer with a thickness of $1.2 \mu\text{m}$, the effective drift time in strong fields was $t_{\text{QWD}} \approx 27$ ps instead of $t_{\text{GaAs}} \approx 13$ ps, expected based on the characteristics of a similar GaAs $p-i-n$

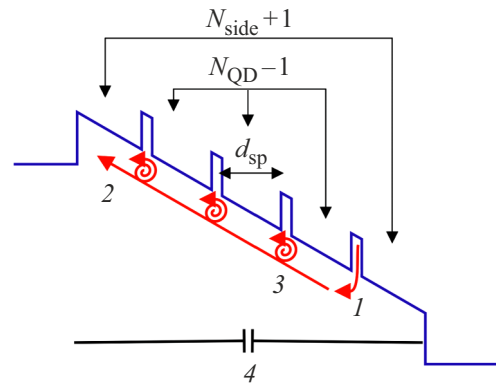


Figure 1. Schematic representation of the valence band of the PD QD ($N_{\text{QD}} = 4$, $N_{\text{side}} = 1$) and processes taken into account in the model that affect the performance: 1 — escape from QD, 2 — drift through i -region, 3 — layer drift delay QD, 4 — recharge of capacity.

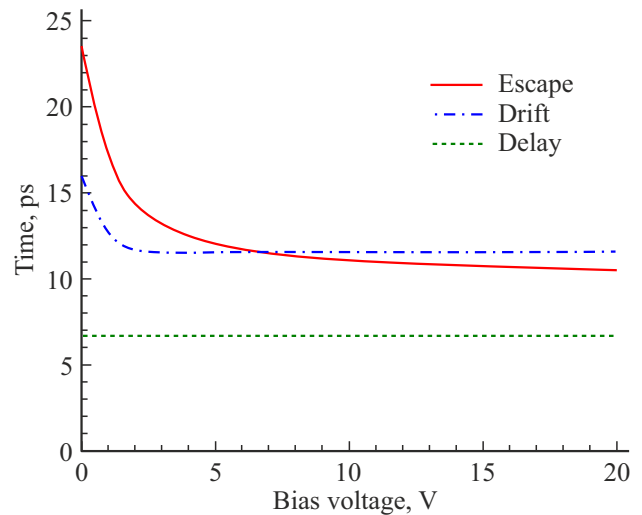


Figure 2. Hole escape time (solid line), drift time (dash-dotted line) and drift delay by 10 layers QD (dashed line). Calculation for $\Phi = 1.4$ V and $d = 1 \mu\text{m}$.

without QWD. Since there are currently no experimental data on the dependence of the delay time on the number of rows of quantum dots, in this work we will be based on the assumption that each additional QD layer leads to an increase in the transfer time by some identical time $t_{\text{delay}} \sim 0.7$ ps, defined as $(t_{\text{QWD}} - t_{\text{GaAs}})/20$. Thus,

$$t_{\text{drift}} = \frac{(N_{\text{QD}} + N_{\text{side}})d_{\text{sp}}}{v_{\text{sat}}} + N_{\text{QD}}t_{\text{delay}}. \quad (2)$$

The response time of the QD PD, set by all processes [13] (escape time, drift, taking into account the delay caused by the multilayer QD structure, as well as the recharging of the RC elements), is equal to

$$t_{\text{resp}} \approx \sqrt{t_{\text{esc}}^2 + t_{\text{drift}}^2 + (2.2t_{\text{RC}})^2}. \quad (3)$$

The factor $2.2(\ln 9)$ takes into account the circumstance that t_{RC} is the time constant of the exponential process, while other times characterize processes that are linear in time. In (3) we do not take into account the process of diffusion of charge carriers produced in the non-depleted regions of the PD structure, since we are interested in the speed only with respect to the light absorbed QD.

The PD capacitance is determined mainly by the capacitance of the p - n junction, which, neglecting the thickness of the depletion areas in the claddings and the edge effects of the strip waveguide, is equal to

$$C = \frac{\varepsilon\varepsilon_0WL}{d}. \quad (4)$$

Here ε — permittivity of the material i -regions, ε_0 — dielectric constant, W and L — width and length of the waveguide PD. At waveguide propagation, the light intensity decreases as $\exp(-\alpha L)$, where $\alpha = N_{QD}\alpha_1$ — modal absorption factor, α_1 — maximum modal absorption by one QD layer at the detection wavelength. Thus, the quantum efficiency, determined by the fraction p of absorbed radiation, changes in proportion to the value of $p = 1 - \exp(-N_{QD}\alpha_1 L)$. Since it is meaningful to compare the characteristics of PD that have the same quantum efficiency for different numbers of QD rows, the length of the waveguide PD should be chosen in accordance with the expression

$$L = \frac{1}{N_{QD}\alpha_1} \ln \frac{1}{1-p}, \quad (5)$$

where the value of p is selected taking into account the required value of the sensitivity (quantum efficiency) of the PD. Let us underline that the value of α_1 depends both on the properties of specific QD and on the position of the detected radiation wavelength relative to the spectral sensitivity maximum. For example, high values of modal absorption (the product of material absorption and the optical confinement factor of the waveguide mode) at the wavelength corresponding to the fundamental optical transition ($> 50 \text{ cm}^{-1}$ per layer at a wavelength of 1060 nm [14]) were reported for InGaAs QWD.

At a sufficiently large reverse bias, the dependence of the PD response time on the parameters of the QD structure of interest to us can be written explicitly as

$$t_{\text{resp}} \approx \sqrt{t_{\infty}^2 + \left[\frac{(N_{QD} + N_{\text{side}})d_{\text{sp}}}{v_{\text{sat}}} + N_{QD}t_{\text{delay}} \right]^2 + \left[\frac{A}{d_{\text{sp}}N_{QD}(N_{QD} + N_{\text{side}})} \right]^2}, \quad (6)$$

where

$$A = 2.2 \ln \left(\frac{1}{1-p} \right) \frac{\varepsilon\varepsilon_0WR}{\alpha_1},$$

R — resistance, determined mainly by the load resistance. As can be seen, the expression contains terms that depend in opposite ways on the number of QD rows and the thickness of the spacer layers: the escape time (the first

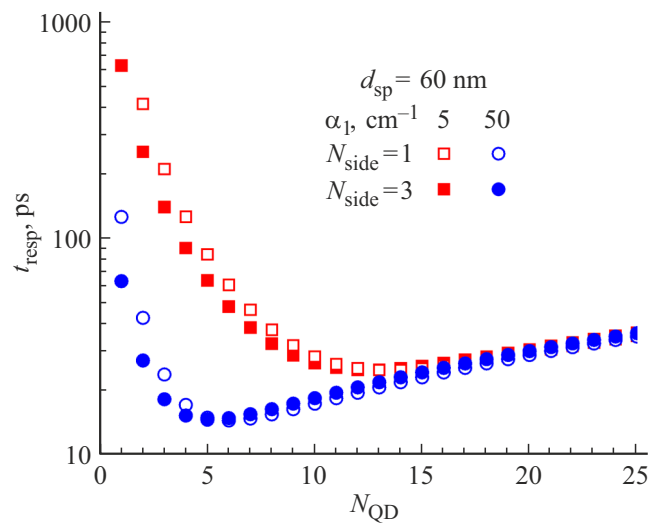


Figure 3. Response time depending on the number of QD rows for different thicknesses of side i -regions (unfilled symbols — $N_{\text{side}} = 1$, filled symbols are $N_{\text{side}} = 3$) and absorption per layer QD (squares — $\alpha_1 = 5 \text{ cm}^{-1}$, circles — $\alpha_1 = 50 \text{ cm}^{-1}$).

term) remains unchanged; the time associated with the transfer of carriers through the depletion region of the PD (the second term) increases, while the time for recharging the capacitance (the third term) decreases with an increase in the number of rows N_{QD} and the thickness of the spacers d_{sp} . This causes the existence of a minimum dependence of t_{resp} on N_{QD} and d_{sp} , which corresponds to the highest performance FD.

3. Results and discussion

The calculation was carried out for the following values of parameters corresponding to PD based on InGaAs QWD in a GaAs matrix: $t_{\infty} = 10 \text{ ps}$, $v_{\text{sat}} = 9 \cdot 10^6 \text{ cm/s}$, $t_{\text{delay}} = 6.7 \text{ ps}$, $\alpha_1 = 5$ or 50 cm^{-1} (corresponding to absorption at the edge or at the maximum spectral sensitivity of QWD), $R = 50 \text{ Ohm}$, $\varepsilon = 12.9$, the value of p was chosen equal to 0.7, $N_{\text{side}} = 1$ or 3, the value of N_{QD} varied in the range of 1–25, d_{sp} from 20 to 100 nm. Calculations, an example of which is presented in Fig. 3, show that the optimal number of N_{QD}^{opt} QD rows, at which the response time reaches its minimum value $t_{\text{resp}}^{\text{min}}$ while other factors being equal, falls within the range achievable for most types of In(Ga)As QDs in matrix GaAs. In any case, this is true for InGaAs QWD, for which high structural perfection and optical quality were reported to be retained up to $N_{QD} = 20$ [15]. Let us note that an increase in the N_{side} value (thickness of the i -side regions) leads to some decrease in t_{resp} for PDs whose light-absorbing region contains a number of QD layers less than N_{QD}^{opt} . However, N_{side} has virtually no effect on either the optimal number of QD rows or the corresponding minimum response time. Meanwhile, the optimal number of QD rows decreases with

an increase in the absorption factor per one QD layer. So, in the case of $\alpha_1 = 5 \text{ cm}^{-1}$, 12–14 layers of QD is optimal, and for $\alpha_1 = 50 \text{ cm}^{-1}$ — 5–6 layers; $t_{\text{resp}}^{\text{min}}$, respectively, decreases from 25 to 15 ps.

The limiting (in terms of -3 dB) response frequency of the PD is related to the response time by the relation $f_{-3 \text{ dB}} = a/t_{\text{resp}}$ [16]. The value of the factor a , which specifies the relationship between the speed parameters in the frequency and time domains, generally speaking, depends on the signal shape (see, for example, [17,18]). Usually its value is assumed to be 0.4. Accordingly, the values of the minimum response obtained in the calculation correspond to the maximum frequency $f_{-3 \text{ dB}}^{\text{max}}$ equal to ~ 16 and $\sim 27 \text{ GHz}$ in the case of $\alpha_1 = 5$ and 50 cm^{-1} , respectively.

Expression (6) allows to explicitly set the required optimal number of QD rows, as well as the maximum PD frequency, depending on other design parameters. Differentiating t_{resp} as per N_{QD} and equating the derivative to zero, we have for the case $N_{\text{QD}} \gg N_{\text{side}}$:

$$N_{\text{QD}}^{\text{opt}} = \left[\sqrt{2} \frac{\frac{A}{d_{\text{sp}}}}{\frac{d_{\text{sp}}}{v_{\text{sat}}} + t_{\text{delay}}} \right]^{1/3}. \quad (7)$$

Substituting (7) in (6), we obtain

$$f_{-3 \text{ dB}}^{\text{max}} = \frac{a}{\sqrt{\left(\frac{1}{2^{2/3}} + 2^{1/3}\right) \left(\frac{A}{d_{\text{sp}}}\right)^{2/3} \left(\frac{d_{\text{sp}}}{v_{\text{sat}}} + t_{\text{delay}}\right)^{4/3} + t_{\infty}^2}}. \quad (8)$$

Analytical expressions (7) and (8) satisfactorily reproduce, taking into account the discrete nature of the number of QD rows, the calculated dependences of the corresponding values on the thickness of the spacer layer, as follows from the data presented in Fig. 4. The optimal

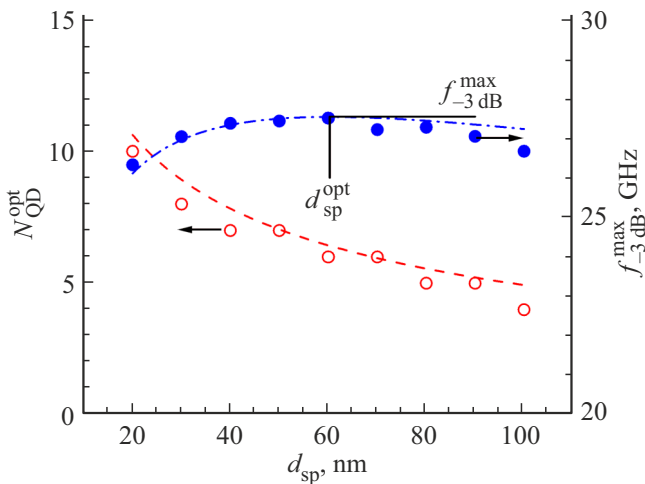


Figure 4. Calculated dependence of the optimal number of QD rows (open symbols) and the corresponding maximum PD frequency (solid symbols) for $\alpha_1 = 50 \text{ cm}^{-1}$ and $N_{\text{side}} = 1$. Lines — approximation with (7) (dashed line), (8) (dash-dotted line) and (10) (solid line).

number of QD rows decreases as d_{sp} increases. For the case of $\alpha_1 = 50 \text{ cm}^{-1}$, the value of $N_{\text{QD}}^{\text{opt}}$ varies from 10 to 4 for the spacer layer thickness range under consideration. Let us underline that such a combination of the number of rows and the thickness of the spacer layers (with the possible exception of only 10 QD rows with 20-nm thick spacer layers) can be realized without detriment to the optical quality of the heterostructure for InGaAs QWD, as well as for most other types In(Ga)As QDs synthesized on GaAs substrates [19,20].

The dependence of $f_{-3 \text{ dB}}^{\text{max}}$ on d_{sp} shows a flat maximum located near $d_{\text{sp}} = 60 \text{ nm}$, at which $f_{-3 \text{ dB}}^{\text{max}}$ reaches 27.5 GHz . The search for the function extremum given by expression (8) allows to establish that the optimal spacer thickness is determined by the product of the saturated carrier velocity and the drift delay time:

$$d_{\text{sp}}^{\text{opt}} = v_{\text{sat}} t_{\text{delay}}, \quad (9)$$

and the limiting frequency corresponding to such a width of the spacer layer

$$f_{-3 \text{ dB}}^{\text{peak}} \equiv f_{-3 \text{ dB}}^{\text{max}}(d_{\text{sp}}^{\text{opt}}) = \frac{a}{\sqrt{\left(2^{2/3} + 2^{5/3}\right) \left(\frac{A t_{\text{delay}}}{v_{\text{sat}}}\right)^{2/3} + t_{\infty}^2}}. \quad (10)$$

For the material parameters used in the calculations, $d_{\text{sp}}^{\text{opt}}$ is 60.3 nm , and $f_{-3 \text{ dB}}^{\text{peak}} = 27.5 \text{ GHz}$. In the limit of very high absorption (which corresponds to $A \rightarrow 0$), the limiting frequency is determined mainly by the escape time from the QD ($f_{-3 \text{ dB}}^{\text{peak}} \rightarrow a/t_1$), and in the limit of low absorption — by a set of parameters characterizing capacitive and transport properties:

$$f_{-3 \text{ dB}}^{\text{peak}} \rightarrow \frac{0.1}{\left(\frac{A t_{\text{delay}}}{v_{\text{sat}}}\right)^{1/3}}.$$

4. Conclusion

Thus, the paper considers the main factors affecting the speed of PD based on multilayer QD: the escape of photogenerated charge carriers from the QD, their transport through the depletion region (including both the time of transfer through the spacer layer and the drift delay introduced by the QD layer). The fact that the characteristic times associated with the last two phenomena depend oppositely on the number of QD rows and the thickness of the spacer layers determines the existence of a minimum in the dependence of the response time on these structural parameters. Analytical expressions are obtained that allow to explicitly determine the optimal values of the thickness of the spacer layer and the number of QD rows. It is shown that, in particular, they depend on the value of the coefficient of modal light absorption per one QD layer. For InGaAs quantum well dots, for which the modal absorption at the maximum spectral sensitivity is $\sim 50 \text{ cm}^{-1}$ per layer, the optimal parameters of the spacer layer thickness 60 nm and

the number of rows 6, which correspond to the maximum speed of the PD with a cutoff frequency at the level -3 dB approximately 27 GHz.

Funding

The studies were carried out as part of the Fundamental Research Program of the National Research University Higher School of Economics. M.V. Maximov, and F.I. Zubov acknowledge project FSRM-2023-0010 of the Ministry of Science and Higher Education of the Russian Federation.

Conflict of interest

The authors declare that they have no conflict of interest.

References

- [1] Y. Wan, Z. Zhang, R. Chao, J. Norman, D. Jung, C. Shang, Q. Li, M.J. Kennedy, D. Liang, C. Zhang, J.-W. Shi, A.C. Gossard, K.M. Lau, J.E. Bowers. *Opt. Express*, **25** (22), 27715 (2017).
- [2] N.V. Kryzhanovskaya, F.I. Zubov, E.I. Moiseev, A.S. Dragunova, K.A. Ivanov, M.V. Maximov, N.A. Kaluzhnyy, S.A. Mintairov, S.V. Mikushev, M.M. Kulagina, J.A. Guseva, A.I. Likhachev, A.E. Zhukov. *Laser Phys. Lett.*, **19** (1), 016201 (2022).
- [3] D. Inoue, Y. Wan, D. Jung, J. Norman, C. Shang, N. Nishiyama, S. Arai, A.C. Gossard, J.E. Bowers. *Appl. Phys. Lett.*, **113** (9), 093506 (2018).
- [4] J. Huang, Y. Wan, D. Jung, J. Norman, C. Shang, Q. Li, K.M. Lau, A.C. Gossard, J.E. Bowers, B. Chen. *ACS Photonics*, **6** (5), 1100 (2019).
- [5] A. Zhukov, S. Blokhin, N. Maleev, N. Kryzhanovskaya, E. Moiseev, A. Nadtochiy, S. Mintairov, N. Kalyuzhnyy, F. Zubov, M. Maximov. *Opt. Express*, **29** (25), 40677 (2021).
- [6] N.V. Kryzhanovskaya, S.A. Blokhin, I.S. Makhov, E.I. Moiseev, A.M. Nadtochiy, N.A. Fominykh, S.A. Mintairov, N.A. Kalyuzhnyy, Yu.A. Guseva, M.M. Kulagina, F.I. Zubov, E.S. Kolodezny, M.V. Maksimov, A.E. Zhukov. *FTP*, **57** (3), 198 (2023). (in Russian).
- [7] B. Tossoun, G. Kurczveil, S. Srinivasan, A. Descos, D. Liang, R.G. Beausoleil. *Optics Lett.*, **46** (16), 3821 (2021).
- [8] X.M. Sun, H. Zhang, H. Zhu, P. Xu, G. R. Li, J. Liu, H.Z. Zheng. *Electron. Lett.*, **45** (6), 329 (2009).
- [9] O. Baklenov, H. Nie, K.A. Anselm, J.C. Campbell, B.G. Streetman. *Electron. Lett.*, **34** (7), 694 (1998).
- [10] W.H. Chang, W.Y. Chen, T.M. Hsu, N.T. Yeh, J.I. Chyi. *Phys. Rev. B*, **66** (19), 195337 (2002).
- [11] V.V. Nikolaev, E.A. Avrutin. *IEEE J. Quant. Electron.*, **39** (12), 1653 (2003).
- [12] I. Pisarenko, E. Ryndin. *Electronics*, **5** (3), 52 (2016).
- [13] A.O. Gouscha, B. Tabbert. *Opt. Eng.*, **56** (9), 097101 (2017).
- [14] A.M. Nadtochiy, N.Yu. Gordeev, A.A. Kharchenko, S.A. Mintairov, N.A. Kalyuzhnyy, Yu.S. Berdnikov, Yu.M. Shernyakov, M.V. Maximov, A.E. Zhukov. *J. Lightwave Technol.*, **39** (23), 7479 (2021).
- [15] S.A. Mintairov, N.A. Kalyuzhnyy, V.M. Lantratov, M.V. Maximov, A.M. Nadtochiy, S.A. Ruvimov, A.E. Zhukov. *Nanotechnology*, **26** (38), 385202 (2015).
- [16] S. Zi. *Fizika poluprovodnikovyk priborov* (M., Mir, 1984) v. 2. (in Russian).
- [17] Si Photodiodes, Technical notes. https://www.hamamatsu.com/content/dam/hamamatsu-photonics/sites/documents/99_SALES_LIBRARY/ssd/si_pd_kspd9001e.pdf
- [18] Insights into High-Speed Detectors and High-Frequency Techniques <https://www.newport.com/n/insights-into-high-speed-detectors-and-high-frequency-techniques>
- [19] I. Krestnikov, D. Livshits, S. Mikhlin, A. Kozhukhov, A. Kovsh, N. Ledentsov, A. Zhukov. *Electron. Lett.*, **41** (24), 1330 (2005).
- [20] A. McWilliam, A.A. Lagatsky, C.T.A. Brown, W. Sibbett, A.E. Zhukov, V.M. Ustinov, A.P. Vasil'ev, E.U. Rafailov. *Optics Lett.*, **31** (10), 1444 (2006).

Translated by E.Potapova